THE MOTION OF SPHERICAL DROPS IN THE FLOW OF A VISCOUS LIQUID

V. Ya. Rivkind, G. M. Ryskin, and G. A. Fishbein

UDC 532.516

We consider the flow of a viscous fluid past a spherical drop at moderate Reynolds numbers. We give the numerical solution of the Navier–Stokes equation for the flow of the liquid inside and outside a drop subject to compatibility conditions at the boundary.

The study of the motion of drops or gas bubbles in liquid media is closely associated with the problem of designing industrial chemical apparatus for many important problems in liquid extraction.

In practice drops move at moderate Reynolds numbers (from several tens to several hundreds). Similar flow conditions have received little study.

This paper is devoted to the solution of the problem of the flow of a viscous liquid past a single drop at moderate Reynolds numbers. It is assumed that the motion is uniform and rectilinear and that the drop retains its spherical form.

The exact solution is known [1, 2] for $Re \ll 1$. On the other hand, for sufficiently large Reynolds numbers the problem of the flow past a gas bubble has been considered within the framework of hydrodynamic boundary layer theory by Levich [3] and Moore [4]. For a liquid drop similar solutions were investigated by Chao [5] assuming that there was a boundary layer at both sides of the boundary of the drop.

For moderate Reynolds numbers an approximate solution was given in [6-9] of the problem of the flow past a solid sphere or a liquid drop using the Galerkin method. A critical review of the solutions obtained by the above authors can be found in [10]. In recent investigations Hamielec and his co-authors [11, 12] discussed the numerical solution of the Navier–Stokes equations for flows with infinite (for a solid sphere) or zero (for a gas bubble) viscosity ratios at Reynolds numbers up to $Re \approx 200$. The solutions obtained showed that the approximate methods of [6-9] were not sufficiently accurate.

Since only approximate solutions [7-9] are known for an arbitrary viscosity ratio (a liquid drop), in this paper we discuss the numerical solution of the Navier–Stokes equations for the flow of a liquid inside and outside a drop subject to compatibility conditions at the boundary. The solution is constructed as a function of three parameters – the Reynolds numbers in the drop and in the surrounding liquid, and the viscosity ratio.

Fundamental Equations and Boundary Conditions. If the origin of coordinates is at the center of the drop and the polar axis lies in the direction of the flow, and we note that, by symmetry, the solution is independent of the azimuthal angle φ, then the Navier–Stokes equations for the stream function $\overline{\Phi}$, in nondimensional variables, are

$$\frac{Re}{2}\left[\frac{\partial\Psi}{\partial\theta}\cdot\frac{\partial}{\partial r}\left(\frac{\zeta}{r\sin\theta}\right)-\frac{\partial\Psi}{\partial r}\cdot\frac{\partial}{\partial\theta}\left(\frac{\zeta}{r\sin\theta}\right)\right]\cdot\sin\theta=E^2(\zeta r\sin\theta), \tag{1}$$

$$E^2\Psi+\zeta r\sin\theta=0, \tag{2}$$

A. A. Zhdanov Leningrad State University, All-Union Scientific Research Institute of Petrochemical Processes, Leningrad. Translated from Inzhenerno-Fizicheskii Zhurnal, Vol. 20, No. 6, pp. 1027-1035, June, 1971. Original article submitted April 24, 1970.

where

$$E^2 = \frac{\partial^2}{\partial r^2} + \frac{\sin\theta}{r^2} \cdot \frac{\partial}{\partial\theta}\left(\frac{1}{\sin\theta} \cdot \frac{\partial}{\partial\theta}\right);$$

r is a nondimensional coordinate in units of the radius of the drop; θ is the polar angle ($0 \leq \theta \leq \pi$).

Equations (1) and (2) hold both inside and outside the drop; the variables relating to the inside region will be denoted by the subscript 1, those for the outside region, by the subscript 2.

Equations (1) and (2) are solved subject to the following boundary conditions:

at the surface of the drop (r = 1):

$$v_{r1} = v_{r2} = 0, \tag{3}$$

$$v_{\theta 1} = v_{\theta 2}, \tag{4}$$

$$(\tau_{r\theta})_1 = (\tau_{r\theta})_2; \tag{5}$$

inside the drop:

$$v_{r1};\ v_{\theta 1}\big|_{r\to 0} \neq \infty; \tag{6}$$

far from the drop the liquid velocity is equal to the velocity of the incident flow:

$$\sqrt{v_{r2}^2 + v_{\theta 2}^2}\Big|_{r\to\infty} \to V_\infty. \tag{7}$$

Here v_r and v_θ, the normal and tangential velocity components of the liquid, are given by the equations

$$v_r = \frac{1}{r^2 \sin\theta} \cdot \frac{\partial\Psi}{\partial\theta}; \quad v_\theta = -\frac{1}{r\sin\theta} \cdot \frac{\partial\Psi}{\partial r};$$

and $\tau_{r\theta}$ is the tangential component of the stress tensor.

The boundary conditions, in terms of Ψ and ζ are:

inner region:

$$\Psi_1 = 0 \text{ on the boundary of the region } (\theta=0;\ \theta=\pi;\ r=0;\ r=1); \tag{8}$$

$$\zeta_1 = 0 \text{ on the axis of symmetry } (\theta=0;\ \theta=\pi;\ r=0); \tag{9}$$

$$\zeta_1\big|_{r=1} = -\frac{1}{\sin\theta} \cdot \frac{\partial^2\Psi_1}{\partial r^2}\bigg|_{r=1}; \tag{10}$$

outer region:

$$\Psi_2 = 0 \quad \text{for} \quad \theta=0;\ \theta=\pi;\ r=1; \tag{11}$$

$$\frac{\Psi_2}{r^2} \to \frac{1}{2}\sin^2\theta \quad \text{for} \quad r\to\infty; \tag{12}$$

$$\zeta_2 = 0 \quad \text{for} \quad \theta=0 \text{ and } \theta=\pi; \tag{13}$$

$$\zeta_2\big|_{r=1} = -\frac{1}{\sin\theta} \cdot \frac{\partial^2\Psi_2}{\partial r^2}\bigg|_{r=1}; \tag{14}$$

$$\zeta_2 \to 0 \quad \text{for} \quad r\to\infty. \tag{15}$$

The compatibility conditions are:

if the liquid does not slip at the boundary:

$$\frac{\partial\Psi_1}{\partial r}\bigg|_{r=1} = \frac{\partial\Psi_2}{\partial r}\bigg|_{r=1}; \tag{16}$$

continuity of tangential components of the stress tensor:

$$\mu\left(2\frac{\partial\Psi_1}{\partial r} - \frac{\partial^2\Psi_1}{\partial r^2}\right)_{r=1} = \left(2\frac{\partial\Psi_2}{\partial r} - \frac{\partial^2\Psi_2}{\partial r^2}\right)_{r=1}, \tag{17}$$

where $\mu = \mu_1/\mu_2$ is the ratio of the coefficients of dynamic viscosity of the inner and outer liquids.

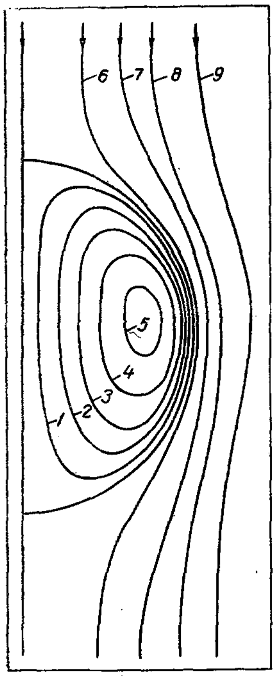

Fig. 1. Streamline pattern at $Re_1 = 50$, $Re_2 = 100$ and $\mu = 1$ (1–$\bar{\Psi}_1 = 0.005$, 2) $\bar{\Psi}_1 = 0.020$, 3) $\bar{\Psi}_1 = 0.040$, 4) $\bar{\Psi}_1 = 0.065$, 5) $\bar{\Psi}_1 = 0.095$, 6) $\bar{\Psi}_2 = 0.020$, 7) $\bar{\Psi}_2 = 0.100$, 8) $\bar{\Psi}_2 = 0.200$, 9) $\bar{\Psi}_2 = 0.400$).

Numerical Solution. The problems can be considered, as in [13, 14], as a problem for equations with discontinuous coefficients. To solve it we use a net point method. First we make the following transformations in the inner region:

1) we introduce the new unknown "perturbation" function Ψ^* such that

$$\Psi = \frac{1}{2} r^2 \sin^2\theta + \Psi^*; \tag{18}$$

2) we make an inversion of the external region in the unit semicircle by means of the coordinate transformation $\rho = 1/r$.

These transformations make it possible to solve the external problem in a finite region with zero value of Ψ^* when $\rho = 0$. The boundary conditions for Ψ^* are

$$\Psi^* = 0 \text{ for } \theta = 0 \text{ and } \theta = \pi; \tag{19}$$

$$\Psi^*\big|_{\rho=1} = -\frac{1}{2}\sin^2\theta; \tag{20}$$

$$\Psi^*\big|_{\rho=0} = 0. \tag{21}$$

Then, in accordance with the finite difference method [15, 16] we write the Eqs. (1) and (2) formally in nonstationary form:

$$\frac{\partial\zeta}{\partial t_1} = \frac{2}{\mathrm{Re}} \cdot \frac{E^2(\zeta r \sin\theta)}{r\sin\theta} + \frac{1}{r}\left[\frac{\partial\Psi}{\partial r} \cdot \frac{\partial}{\partial\theta}\left(\frac{\zeta}{r\sin\theta}\right) - \frac{\partial\Psi}{\partial\theta} \cdot \frac{\partial}{\partial r}\left(\frac{\zeta}{r\sin\theta}\right)\right]; \tag{22}$$

$$\frac{\partial\Psi}{\partial t_2} = E^2\Psi + \zeta r \sin\theta. \tag{23}$$

We introduce the time step lengths τ_1 and τ_2 for the time t_1 and t_2, so that $t_{1n} = n\tau_1$, $t_{2n} = n\tau_2$, where $n = 0, 1, 2, \ldots$. We choose the step length in the angular coordinate as the constant $\sigma = \pi/M$; $\theta_k = \sigma k$, $k = 0, 1, \ldots, M$. In the coordinates r and ρ we choose variables so that

$$r_i = \sum_{j=0}^{i-1} g_j,\quad g_i = r_{i+1} - r_i,\quad i = 0, 1, 2, \ldots, N,$$

$$\rho_i = \sum_{j=0}^{i-1} h_j,\quad h_i = \rho_{i+1} - \rho_i;\quad i = 0, 1, 2, \ldots, E.$$

Following the decoupling scheme we have chosen we arrive at a difference formulation of the problem: for the inner region:

$$\frac{\zeta_{i,k}^{n+\frac{1}{2}}-\zeta_{i,k}^{n}}{\tau_1}=\frac{2}{\mathrm{Re}_1}\cdot\frac{\delta^2\zeta_{i,k}^{n+\frac{1}{2}}}{\delta r^2}+\frac{1}{r_i}\left(\frac{2}{\mathrm{Re}_1}-\frac{1}{r_i\sin\theta_k}\cdot\frac{\delta\Psi_{i,k}^{n}}{\delta\theta}\right)$$

$$\times\frac{\delta\zeta_{i,k}^{n+\frac{1}{2}}}{\delta r}+\frac{1}{r_i^3\sin\theta_k}\cdot\frac{\delta\Psi_{i,k}^{n}}{\delta\theta}\zeta_{i,k}^{n+\frac{1}{2}}; \tag{24}$$

$$\frac{\zeta_{i,k}^{n+1}-\zeta_{i,k}^{n+\frac{1}{2}}}{\tau_1}=\frac{1}{r_i^2}\left[\frac{2}{\mathrm{Re}_1}\cdot\frac{\delta^2\zeta_{i,k}^{n+1}}{\delta\theta^2}+\frac{1}{\sin\theta_k}\left(\frac{2\cos\theta_k}{\mathrm{Re}_1}+\frac{\delta\Psi_{i,k}^{n}}{\delta r}\right)\frac{\delta\zeta_{i,k}^{n+1}}{\delta\theta}-\frac{1}{\sin^2\theta_k}\left(\frac{2}{\mathrm{Re}_1}+\cos\theta_k\frac{\delta\Psi_{i,k}^{n}}{\delta r}\right)\zeta_{i,k}^{n+1}\right] \tag{25}$$

$$\frac{\Psi_{i,k}^{n+1}-\Psi_{i,k}^{n}}{\tau_2}=\frac{\delta^2\Psi_{i,k}^{n+\frac{1}{2}}}{\delta r^2}+\lambda_1\zeta_{i,k}^{n+1}r_i\sin\theta_k; \tag{26}$$

$$\frac{\Psi_{i,k}^{n+1}-\Psi_{i,k}^{n+\frac{1}{2}}}{\tau_2}=\frac{1}{r_i^2}\left[\frac{\delta^2\Psi_{i,k}^{n+1}}{\delta\theta^2}-\mathrm{ctg}\,\theta_k\frac{\delta\Psi_{i,k}^{n+1}}{\delta\theta}\right]+(1-\lambda_1)r_i\sin\theta_k\zeta_{i,k}^{n+1}. \tag{27}$$

For the outer region in the variables ρ and θ we have:

$$\frac{\zeta_{i,k}^{n+\frac{1}{2}}-\zeta_{i,k}^{n}}{\tau_1}=\frac{2\rho_i^4}{\mathrm{Re}_2}\cdot\frac{\delta^2\zeta_{i,k}^{n+\frac{1}{2}}}{\delta\rho^2}+\rho_i^2\left(\frac{\rho_i^2}{\sin\theta_k}\cdot\frac{\delta\Psi_{i,k}^{*n}}{\delta\theta}+\cos\theta_k\right)\frac{\delta\zeta_{i,k}^{n+\frac{1}{2}}}{\delta\rho}+\frac{\rho_i^3}{\sin\theta_k}\cdot\frac{\delta\Psi_{i,k}^{*n}}{\delta\theta}\zeta_{i,k}^{n+\frac{1}{2}}; \tag{28}$$

$$\frac{\zeta_{i,k}^{n+1}-\zeta_{i,k}^{n+\frac{1}{2}}}{\tau_1}=\frac{2\rho_i^2}{\mathrm{Re}_2}\cdot\frac{\delta^2\zeta_{i,k}^{n+1}}{\delta\theta^2}+\rho_i\left(\frac{2\rho_i}{\mathrm{Re}_2\,\mathrm{tg}\,\theta_k}+\sin\theta_k-\frac{\rho_i^3}{\sin\theta_k}\cdot\frac{\delta\Psi_{i,k}^{*n}}{\delta\rho}\right)\frac{\delta\zeta_{i,k}^{n+1}}{\delta\theta}$$

$$-\frac{\rho_i^2}{\sin^2\theta_k}\left(\frac{2}{\mathrm{Re}_2}-\rho_i\cos\theta_k\frac{\delta\Psi_{i,k}^{*n}}{\delta\rho}\right)\zeta_{i,k}^{n+1}, \tag{29}$$

$$\frac{\Psi_{i,k}^{*n+\frac{1}{2}}-\Psi_{i,k}^{*n}}{\tau_2}=\rho_i^4\frac{\delta^2\Psi_{i,k}^{*n+\frac{1}{2}}}{\delta\rho^2}+2\rho_i^3\frac{\delta\Psi_{i,k}^{*n+\frac{1}{2}}}{\delta\rho}+\lambda_2\frac{\sin\theta_k}{\rho_i}\zeta_{i,k}^{n+1}, \tag{30}$$

$$\frac{\Psi_{i,k}^{*n+1}-\Psi_{i,k}^{*n+\frac{1}{2}}}{\tau_2}=\rho_i^2\frac{\delta^2\Psi_{i,k}^{*n+1}}{\delta\theta^2}-\frac{\rho_i^2}{\mathrm{tg}\,\theta_k}\cdot\frac{\delta\Psi_{i,k}^{*n+1}}{\delta\theta}+(1-\lambda_2)\frac{\sin\theta_k}{\rho_i}\zeta_{i,k}^{n+1}, \tag{31}$$

where $f(r_i, \theta_k, t_n) = f_{i,k}^n$; λ_1, and λ_2 are parameters defined in the interval [0, 1]; $\delta/\delta\theta$; $\delta/\delta r$; $\delta/\delta\rho$; $\delta^2/\delta\theta^2$; $\delta^2/\delta r^2$; $\delta^2/\delta\rho^2$ are three-point difference derivatives. The first order derivatives are weighted, for example,

$$\frac{\delta f_{i,k}^{n}}{\delta\theta}=m\frac{f_{i,k+1}^{n}-f_{i,k}^{n}}{\sigma}+(1-m)\frac{f_{i,k}^{m}-f_{i,k-1}^{m}}{\sigma}, \tag{32}$$

where $0 \le m \le 1$.

The boundary conditions (8), (19), (20), (13), and (15) are approximated by specifying Ψ and ζ on the boundary lines of the net. The boundary conditions (10) and (14), together with (16) and (17) are approximated as follows.

Suppose we know Ψ on some line. To obtain the boundary condition for ζ on the following line we have to calculate $\partial\Psi_1/\partial r|_{r=1}$, $\partial\Psi_2/\partial r|_{r=1}$, $\partial^2\Psi_1/\partial r^2|_{r=1}$, and $\partial^2\Psi_2/\partial r^2|_{r=1}$. But in calculating, for example, $\partial\Psi_1/\partial r|_{r=1} = \delta_1^*$ and $\partial\Psi_2/\partial r|_{r=1} = \delta_2^*$ directly from the results on the known line, it may happen that condition (19) does not hold.

Hence, here we use the following iteration process: we choose δ_1, δ_2, and an additional parameter $\gamma (0 \le \gamma \le 1)$ so that

$$\gamma\delta_1+(1-\gamma)\delta_2=\gamma\delta_1^*+(1-\gamma)\delta_2^*,$$
$$\delta_1=\delta_2. \tag{33}$$

If the values of the stream function in the given line satisfy (16), the parameter γ is unnecessary. If not, we choose some intermediate value of $\delta (\delta_1 = \delta_2 = \delta)$:

$$\delta=\gamma\delta_1^*+(1-\gamma)\delta_2^*. \tag{34}$$

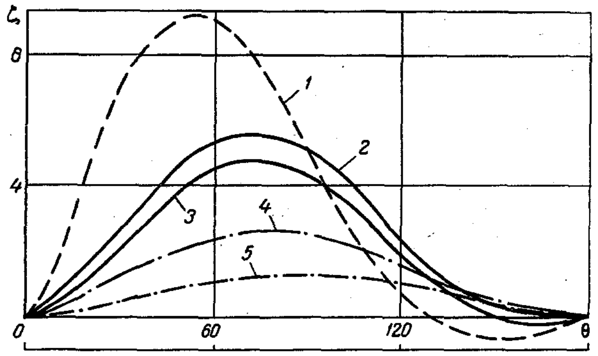

Fig. 2. Vorticity distribution at the surface of the sphere (1) the Hamielec solution [11] for a solid sphere at $Re_2 = 100$; 2, 3) the solution obtained in this paper for a liquid drop at $Re_1 = 50$, $Re_2 = 100$, $\mu = 1$ and $Re_1 = 100$, $Re_2 = 200$, $\mu = 1$; 4) the Hamielec solution [11] for a gas bubble at $Re_2 = 100$; 5) the Hadamard solution [1] for $\mu = 1$. θ in deg.

We find δ_1^* and δ_2^* from a Taylor expansion in the neighborhood of the boundary and the values of the stream function on two lines of the net nearest the boundary. Thus, for the inner region we have

$$\delta_1^* = \frac{g_{N-1}^2 \Psi_{N-2} - (g_{N-2} + g_{N-1})^2 \Psi_{N-1}}{g_{N-2}\, g_{N-1} (g_{N-2} + g_{N-1})}. \qquad (35)$$

Conditions (10) and (14), in conjunction with (17) are approximated in accordance with the same principle. As a result of this process, the compatibility conditions are automatically satisfied as $t \to \infty$

The solution is calculated as follows. From the known values of Ψ on the preceding line we calculate ζ_1 and ζ_2 on the boundary for the new line. Then separately, in the inner region, from equations (24)-(27), and in the outer region, from equations (28)-(31), we determine successively ζ on the $(n + 1/2)$ line and Ψ on the $(n + 1)$ line. Then the calculation is repeated. Equations (24)-(31) are solved by the method of iteration.

The above algorithm was written as a program in ALGOL 60 and translated by the translator TA-IM. The calculations were carried out on a BÉSM-4 computer. For the first calculations the initial line was taken as the Hadamard solution [1], obtained as the solution of the equation $E^2(E^2\Psi)$. The step length in the radial coordinate was variable, being refined at the liquid boundary. Thus, for example, in the outer region

$$\rho_i = \sin\frac{\pi i}{2E}, \quad i=0,1,\ldots, E.$$

To verify that the method could be applied over a wide range of Reynolds numbers, a variant with the parameters $Re_1 = 100$, $R\hat{e}_2 = 200$, $\mu = 1$ and initial line corresponding to the Hadamard solution for $\mu = 1$ was first computed.

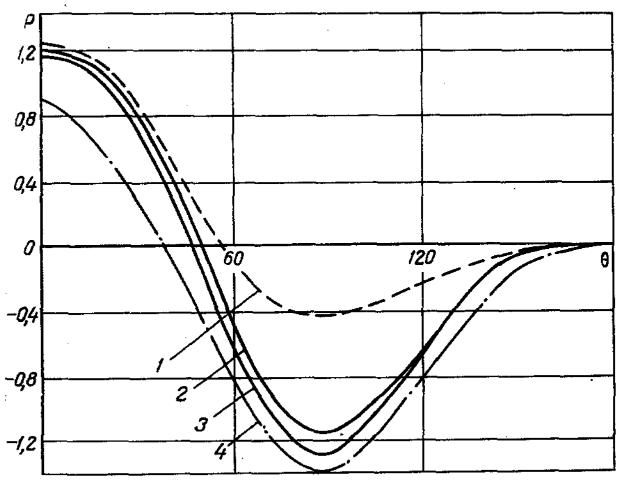

Fig. 3. Pressure distribution at the surface of the sphere (1) the Hamielec solution [11] for a solid sphere at $Re_2 = 100$; 2, 3) the solution obtained in this paper for a liquid drop at $Re_1 = 50$, $Re_2 = 100$, $\mu = 1$ and $Re_1 = 100$, $Re_2 = 200$, $\mu = 1$; 4) the Hamielec solution [11] for a gas bubble at $Re_2 = 100$. θ in deg.

Because of the restrictions imposed by the BÉSM-4, a quite coarse net ($M = N = E = 10$) was chosen. This prevented us from determining the position of the point of flow breakaway or the drag coefficient to a sufficient degree of accuracy. For a more exact solution of the problem we have to used a refined net and computers of higher speed.

DISCUSSION OF RESULTS

The results of the numerical calculations are shown in Figs. 1-5. Fig. 1 shows the streamline pattern for flows in a moving drop and in the surrounding medium at $Re_1 = 50$, $Re_2 = 100$, $\mu = 1$. We note that the geometry of the inner flow at $Re \approx 100$ is little different from the Hadamard flow ($Re < 1$). Some flow asymmetry is observed. The center of circulation of the liquid is displaced by approximately 8° towards the incident flow. The maximum value of the stream function in the inner region increases approximately three times by comparison with the Hadamard solution for $\mu = 1$, which corresponds to a more intense circulation of the liquid. A weak asymmetry in the external flow is also noticed and the stream line departs from the sphere at the rear.

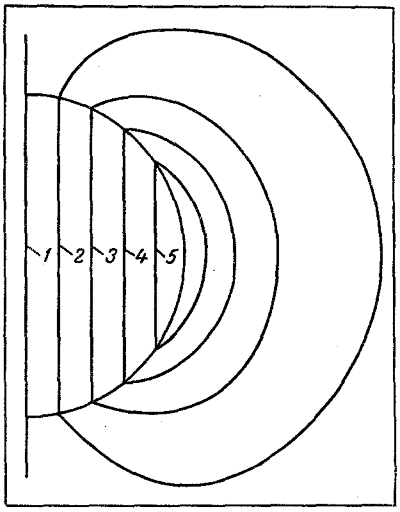

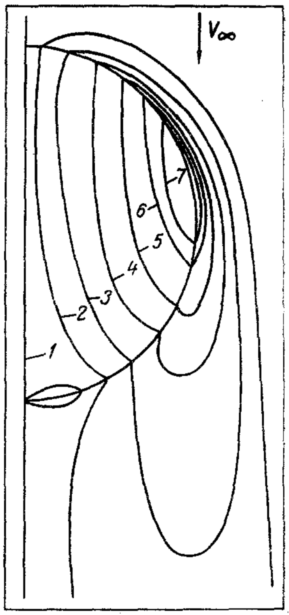

Fig. 4

Fig. 5

Fig. 4. Vortex intensity distribution for the Hadamard solution [1] for $\mu = 1$ ($\zeta_1 = \zeta_2 = \zeta$): 1) $\zeta = 0$, 2) $\zeta = 0.25$, 3) $\zeta = 0.50$, 4) $\zeta = 0.75$, 5) $\zeta = 1.00$.

Fig. 5. Vortex intensity distribution for $Re_1 = 50$, $Re_2 = 100$, $\mu = 1$ ($\zeta_1 = \zeta_2 = \zeta$): 1) $\zeta = 0$, 2) $\zeta = 0.25$, 3) $\zeta = 0.75$, 4) $\zeta = 1.50$, 5) $\zeta = 2.50$, 6) $\zeta = 3.50$, 7) $\zeta = 4.00$.

Figures 2 and 3 show the vorticity and pressure distributions at the surface of the drop for $Re_1 = 50$, $Re_2 = 100$, $\mu = 1$, and $Re_1 = 100$, $Re_2 = 200$, $\mu = 1$ compared with Hamielec's results [11] for a solid sphere and a gas bubble at $Re_2 = 100$. The comparison is made under the condition that the stagnation point is taken as the origin for measuring the polar angle and that the origin for the pressure is at the rear point. As is to be expected, the pressure and vorticity distribution curves at the surface of a liquid drop lie between those corresponding to the limiting cases of a solid sphere and a gas bubble.

Figures 4 and 5 give the vortex intensity distributions (lines ζ = const) for Re < 1 and $\mu = 1$ for the Hadamard solution and as computed in this paper for $Re_1 = 50$, $Re_2 = 100$, $\mu = 1$. Since $\mu = 1$ in the examples quoted, the lines corresponding to a single value of ζ in different regions are closed on the sphere.

It follows from the calculations that the maximum vorticity on the boundary is displaced in the direction of the incident flow, increasing in absolute value by a factor of almost four. Comparing Figs. 4 and 5, we note that as Re increases, the vortex intensity drifts downstream.

The concentration of vortex intensity in a thin strip at the leading surface of the sphere indicates the tendency of the formation of a boundary layer around the drop at moderate Re. Conversely, inside the drop the distribution of vortex intensity is such that no similar tendency is detected.

NOTATION

r	is the radial coordinate;
θ	is the polar angle;
v_r, v_θ	are the radial and tangential velocity components of the liquid;
$\tau_{r\theta}$	is the tangential component of the stress tensor;
$Re = 2V_\infty a/\nu$	is the Reynolds number;
V_∞	is the velocity of the incident flow;
$\nu = \mu/\rho$	is the coefficient of kinematic viscosity;
μ	is the coefficient of dynamic viscosity;
ρ	is the density;
a	is the drop radius;

Ψ	is the stream function;
ζ	is the vorticity;
τ_1, τ_2	are the time step lengths;
σ	is the angular step length;
g, h	are the radius step lengths;
E, N, M	are the numbers of lines of the net;
γ, λ, m	are the parameters of the difference scheme.

Subscripts

1	denotes the inner region of the drop;
2	is the outer region;
i, k	are the numbers of the lines in the net.

LITERATURE CITED

1. J. Hadamard, J. Comptes Rend., 152, p. 1735 (1911).
2. W. Rybozynski, Bull. Acad. Cracovie, A 40 (1911).
3. V. G. Levich, Physicochemical Hydrodynamics [in Russian], Fizmatgiz, Moscow (1959).
4. D. W. Moore, J. Fluid Mech., 16, 161 (1963).
5. B. T. Chao, Phys. of Fluids, 5, 69 (1962).
6. M. Kawaguti, Rept. Inst. Sci. Tokyo, 2 (5/6): 66 (1948).
7. A. E. Hamielec and A. I. Johnson, Can. J. Chem Eng., 40, 41 (1962).
8. A. E. Hamielec, S. H. Storey, and J. M. Whiteherd, Can. J. Chem. Eng., 41, 246 (1963).
9. Y. Nakano and C. Tien, Can. J. Chem. Eng., 45, 135 (1967).
10. B. I. Brounshtein and G. A. Fishbein, in Papers on the Thermodynamics and Kinetics of Chemical Processes [in Russian] GIPKh, No. 66, Khimiya, Leningrad (1970), 66.
11. A. E. Hamielec, T. W. Hoffman, and L. L. Ross, A. I. Ch. E. Journ., 13, 212 (1967).
12. A. E. Hamielec, A. I. Johnson, and W. T. Houghton, A. I. Ch. E. Journ., 13, 220 (1967).
13. O. A. Ladyzhenskaya, Mathematical Problems in the Dynamics of a Viscous Liquid [in Russian], Fizmatgiz, Moscow (1962).
14. V. Ya. Rivkind and N. N. Ural'tseva, Dokl. Akad. Nauk SSSR, 185, No. 2, 271 (1969).
15. L. M. Simuni, Zhurn. Prikl. Mekhan. i Tekhn. Fiziki, No. 6, 106 (1965).
16. T. V. Kuskova, Computational Methods and Programming [in Russian], No. 7, MGU (1967).